Calcif Tissue Int (2006) 78:241–247
DOI: 10.1007/s00223-005-0294-2

Calcified Tissue International

Effects of Lanthanum on Composition, Crystal Size, and Lattice Structure of Femur Bone Mineral of Wistar Rats

J. Huang,[1] T.-L. Zhang,[2] S.-J. Xu,[1] R.-C. Li,[1] K. Wang,[1] J. Zhang,[3] Y.-N. Xie[3]

[1]Department of Chemical Biology, Peking University School of Pharmaceutical Sciences, 38 Xueyuan Road, Beijing 100083, People's Republic of China
[2]School of Pharmaceutical Sciences, Capital University of Medical Sciences, 10 Xitoutiao, You An Men, Beijing 100054, People's Republic of China
[3]Laboratory of Beijing Synchrotron Radiation, Institute of High Energy Physics, Chinese Academy of Sciences, Beijing 100039, People's Republic of China

Received: 7 December 2005 / Accepted: 10 January 2006 / Online publication: 13 April 2006

Abstract. The application of lanthanum (La) in industry, medicine, and agriculture may cause accumulation of the element in human body. This article examines the effects of La on the femur bone mineral of male Wistar rats after administration of $La(NO_3)_3$ by gavage at the dose of 2.0 mg $La(NO_3)_3 \cdot kg^{-1} \cdot day^{-1}$ over a 6-month period. Chemical analysis confirmed La accumulation in bone and loss in bone mineral. Thermogravimetric analysis showed a decrease in the mineral-to-matrix ratio and an increase in carbonate content. Fourier-transform infrared spectrometry revealed elevation in the contents of labile carbonate and acidic phosphate. The synchrotron radiation small-angle X-ray scattering study presented a smaller mean thickness of the mineral crystals in the bone of La-treated rats. The synchrotron radiation-extended X-ray absorption fine structure analysis indicated that the La treatment resulted in a lowered disorder in the crystals. The smaller size, more adsorbed labile carbonate, and more acidic phosphate made the bone mineral easier to dissolve, as revealed in the kinetic measurement of bone demineralization. These findings suggest that La retards bone maturation of rats.

Key words: Lanthanum — Bone mineral — Crystal size — Lattice structure — Rat

The biological effects of rare earth elements (REs) have drawn much attention from chemical, biological, medical, and toxicological circles [1]. REs can be taken in by humans through foodstuffs and medical agents. Although they do not cause any serious toxicosis in most parts of the world due to a low uptake into plants and a subsequent low uptake from the gastrointestinal tract [2], situations might be quite different in some mining areas, where the contents of REs in plants [3], animals [4], and humans [5] are markedly higher. Besides, RE-containing fertilizers have been used to improve the yield and quality of several kinds of crops in China since the 1970s, and RE-containing forage additives have also been on trial in aquaculture and livestock raising since the 1990s [6, 7]. In addition, some RE compounds have exhibited properties that appear promising for medical uses [8, 9]. Most recently, lanthanum (La) carbonate has been used for the treatment of hyperphosphatemia in renal failure and dialysis patients [10, 11]. Consequently, the chance has greatly increased for entrance of REs into the human body.

La is the first element of the lanthanide series, and bone is one of the main sites where La accumulates [12]. La has been recognized as a "bone-seeking" element [13] due to the analogy between La^{3+} and Ca^{2+} [14] in ionic radii [15, 16] and coordination tendency. Further, phosphate ions available from the blood were sufficient for the formation of the very insoluble $LaPO_4$ ($pKsp = 26.15$) [17]. The accumulated La^{3+} in bone mineral may either enter crystal lattice of hydroxyapatite (HAP) or just deposit on crystal surface. Since bone is a metabolically active tissue undergoing continuous remodeling consisting of osteoblastic bone formation and osteoclastic resorption, La^{3+} may affect bone mineral through interfering with cellular activities. In assessing the effect of La on bone, a low-dose, long-term experiment would be desired to make the conclusion more relevant to actual environmental situations.

The purpose of the present study was to examine the La-caused consequence in bone mineral of Wistar rats after administration of $La(NO)_3$ by gavage at the dose of 2.0 mg $La(NO_3)_3 \cdot kg^{-1} \cdot day^{-1}$ for 6 months. We characterized bone samples with techniques such as thermogravimetric (TG) analysis, synchrotron radiation small-angle X-ray scattering (SR-SAXS) spectrometry, Fourier-transform infrared microspectrometry

Correspondence to: T.-L. Zhang; E-mail: tlzhangcums@yahoo.com.cn

(FT-IRM), and synchrotron radiation-extended X-ray absorption fine structure (SR-EXAFS) analysis and measured the demineralization kinetics of bone powder with the pH-stat technique. Alterations have been detected in the content, composition, crystal mean thickness, lattice structure, and dissolution property of femur bone mineral of La-treated Wistar rats. These findings allow us to assess the impact of La on bone maturation.

Materials and Methods

Sample Preparation

The protocol of animal experiments was approved by the Institutional Animal Care and Use Committee at the Peking University Health Science Center. Twenty male Wistar rats, 3 months old, were randomly assigned to two groups: (1) water-treated group as the control and (2) group treated orally with 2.0 mg $La(NO_3)_3 \cdot kg^{-1} \cdot day^{-1}$ for 6 months. At the termination of the study, two femurs from each animal were dissected and cleaned of soft tissue, periosteum, and bone marrow. The right femurs were dehydrated in increasing ethanol concentrations and embedded in polymethylmethacrylate. For FT-IRM analyses, sections of 5-10 μm were cut longitudinally from femur diaphysis. The left femurs were frozen in liquid nitrogen, lyophilized, and ground into powder at liquid nitrogen temperature. Aliquots of bone powder were sieved to a mean diameter of 0.45-0.90 mm and used for kinetic measurement. The specific surface area of the powder was determined by N_2 adsorption (Brunauer-Emmet-Teller single-point method) using an ASAP2010 volumetric adsorption analyzer (Micromeritics Instrument, Norcross, GA, USA). The remaining samples were ground to a fine powder and utilized for other analysis. Tissue lipid in both the sections and bone powders was removed by extraction with a methanol-chloroform mixture (1:2, v/v). Samples from La-treated animals, as well as from controls, were investigated in a blinded study.

Chemical Analysis

Approximately 10 mg of bone power was digested in a nitric acid-perchloric acid mixture (6:1, v/v). Contents of Ca and La were determined by inductively coupled plasma mass spectrometry (ICP-MS) on a Perkin-Elmer (Norwalk, CT) ELAN5000. The phosphorus content was determined using the phosphomolybdate-ascorbic acid method [18]. The mineral content (expressed as mineral-to-matrix ratio, w/w) and the percentage of carbonate (expressed as CO_3%, w/w) in bone were determined by TG analysis [19] with a SDT2960 (System TA, New Castle, DE, USA) apparatus. The heating rate was $10°C \cdot min^{-1}$ from room temperature to 1,000°C. Samples of 10–20 mg were used in each measurement.

SR-SAXS Measurement

A synchrotron X-ray source was used to increase the resolution of SAXS measurement. The experiment was performed at beamline 4B9A of the Beijing Synchrotron Radiation Facility (BSRF). The storage ring was run at 2.2 GeV with electron current 80 mA. A double-crystal Si^{111} monochromator was used to select the X-ray wavelength λ of 0.154 nm. The background scattering and absorption of the samples were corrected. The scattered intensity I(q) was recorded as a function of the scattering vector q, which is related to the scattering angle θ by $q = 2\pi \sin(\theta/\lambda)$. The function I(q) typically contains information on the average size, orientation, and arrangement of mineral crystal in bone. The mean crystal thickness was calculated according to the procedures described by Fratzl et al. [20].

FT-IRM

Infrared spectra were recorded on a Nicolet Magna 750-II spectrometer equipped with a Nic-Plan™ IR microscope. Data were collected in transmission mode, 128 scans per point at 4 cm^{-1} resolution. The measurement was in the range of 4,000–650 cm^{-1} and performed at random positions in the bone using a 20 × 20 μm aperture.

Infrared vibrations of both the mineral and the matrix phases were monitored simultaneously. The mineral phosphate moiety appears in two spectral regions: 650–500 cm^{-1} (sharp) and 1,200–900 cm^{-1} (broad). Only the latter is accessible in studies of mineralized tissues using an FT-IRM instrument with a mercury-cadmium-telluride detector. Curve fitting was carried out on the phosphate ν_1 and ν_3 vibrations (1,200–900 cm^{-1}) and the carbonate ν_2 vibrations (900–845 cm^{-1}) in the spectra using a method described by Boskey et al. [21]. Positions of the peaks were obtained from second derivative spectra and allowed to vary within ± 2 cm^{-1}. The output of this analysis was expressed as a peak position and the related area percentage. Three spectra from separate bones were used for preliminary statistical analysis.

SR-EXAFS Spectrometry

To detect the coordination environment of calcium atoms in bone mineral, SR-EXAFS spectrometry can be employed, as described by Harries et al. [22]. EXAFS spectroscopy is an element-specific technique that can be used to probe the local structure around a certain atom even in a complex microenvironment. The experiment was performed at the beamline of 1W1B of BSRF using a double-crystal Si^{111} monochromator. The storage ring energy was operated at 2.2 GeV with electron current of about 80 mA. To suppress the unwanted harmonics, a detuning of 30% was performed between the two monochromator crystals. The incident and output beam intensities were monitored and recorded using a nitrogen gas flowing ionization chamber. The spectra were scanned in the range of 3.8-5.0 KeV, which covers the *k*-edge absorption of calcium atoms. Energy resolution was about 2.0 eV for the EXAFS. Normalization, background subtraction, and analysis of the EXAFS spectra were done using the Darebury library program EXCURV88 (Darebury Laboratory, Warrington, Cheshire, UK) [23]. A threshold energy (i.e., energy at which the value of the photoelectron wave vector k was 0) of 4,038 eV was used. Spectra were weighted by k^3 to compensate for damping of oscillations at high k. Normalized EXAFS spectra were filtered over a k range of 2.5-9.0 $Å^{-1}$ depending on data quality and Fourier-transformed. The coordination number for each shell was fixed to the value of crystalline HAP so that the values of radial distances (R) and Debye-Waller factors (σ^2) could be estimated.

Measurement of Dissolution Kinetics of Bone Mineral

The pH-stat technique described by Grynpas and Cheng [24] was employed. A volume of 100 mL 150 $mmol \cdot L^{-1}$ KCl, as the working solution, was added into a water-jacked Pyrex cell and warmed to 37.0 ± 0.2°C. Under magnetic stirring at constant speed, the working solution was titrated to pH 4.0 with 100 $mmol \cdot L^{-1}$ acetic acid (HAc). Bone powder of 10.0 ± 0.2 mg was then added and followed immediately by timing. The pH of the solution was then kept constant by addition 100 $mmol \cdot L^{-1}$ HAc under the control of a pH autotitrator (ZD-2, Shanghai Analytical Instrument Co., Shanghai, China) equipped with a combinational glass electrode (E201-C9, Shanghai). In maintaining the pH, the consumed volume of HAc solution was

Table 1. Chemical composition of bone mineral in femur of Wistar rats (data shown as means ± SEM)

	Chemical analysis (n = 10)				TG analysis (n = 10)	
Sample	La (ng/g)	Ca (%)	P (%)	Ca:P (molar)	CO_3^{2-} (%)	Mineral:matrix (w/w)
Normal	6.6 ± 0.4	24.9 ± 0.6	11.4 ± 0.6	1.69 ± 0.08	4.4 ± 0. 3	5.0 ± 0.3
La-treated	22 ± 1*	22.0 ± 0.8*	9.5 ± 0.4[a]	1.83 ± 0.11	6.2 ± 0. 4*	4.5 ± 0.2*

*Significantly different from normal bone, $P < 0.05$

recorded, indicating the extent of bone dissolution. An ion analyzer (PXSJ-216, Shanghai) was used to monitor the change in Ca^{2+} concentration.

Statistical Analysis

Data were expressed as mean ± standard error of the mean (SEM) and statistically assessed by one-way analysis of variance. Difference between the treated and control groups was evaluated by Scheffe's test. $P < 0.05$ was considered significant.

Results

Composition and Crystal Size of Bone Mineral

As presented in Table 1, the amount of La found in the bone of La-treated rats is about three times that in normal bone. The percentages of both Ca and P are slightly reduced (with significance $P < 0.05$), whereas the change in the molar ratio of Ca to P is not significant ($P > 0.05$).

Data derived from TG measurement are also listed in Table 1. The mineral-to-matrix ratio of the bone from La-treated rats decreased, while the percentage of carbonate increased.

The average value of crystal thickness (T) is defined as the smallest dimension of the crystallite and derived from the ratio of volume to surface, which does not require any assumption about shape, monodispersity, or uniform habit of the crystals [25]. Values of T from SR-SAXS measurements were 2.56 ± 0.04 nm (n = 10) for normal bone and 2.42 ± 0.04 nm (n = 10) for La-treated Wistar rats. The difference between the values is significant ($P < 0.05$).

Individual peaks in the 1,800-800 cm^{-1} region of FT-IRM spectra were baseline-corrected and are demonstrated in Figure 1A. The absorbance that arises from mineral phosphate ν_1 and ν_3 vibrations and carbonate (CO_3^{2-}) ν_2 vibrations was identified.

Curve-fitting the ν_2 vibrations (900-845 cm^{-1}) of CO_3^{2-} resulted in three subpeaks that had previously been assigned [26–28]: type A, a peak at 877 cm^{-1}, corresponding to CO_3^{2-} substituted for apatite hydroxyl; type B, a peak at 871 cm^{-1}, for CO_3^{2-} substituted for apatite phosphate; and a peak at 867 cm^{-1} for nonlattice, adsorbed CO_3^{2-} at labile positions of a mineral crystal. As shown in Figure 1B, the content of labile carbonate was significantly higher in the bone mineral phase of La-treated rats than that of normal bone (+12.3%, $P < 0.05$), whereas the carbonate contents of both type A and type B were diminished (type A −5.2%, $P < 0.05$; type B −7.2 %, $P < 0.05$).

The data resolved from curve-fitting in the phosphate ν_1, ν_3 region at 1,180-900 cm^{-1} [29] are presented in Figure 1C. The area percentages of the subpeaks at 1,075 cm^{-1} and 1,145 cm^{-1} are proportional to crystal size and content of the acidic phosphate (HPO_4^{2-}) [26, 30], respectively. The acidic phosphate increased in La-treated bone. A smaller size with the La-treated bone was derived from the peak at 1,075 cm^{-1}, consistent with the results from the SR-SAXS experiment.

Microstructure of Bone Minerals

The lattice parameters obtained from the SR-EXAFS experiment are listed in Table 2. Due to the complexity of the structure of HAP crystal, only average values of the coordination bond distances for local Ca^{2+} can be derived. The calcium-neighbor distances (R) of the two kinds of bone samples were almost identical to that of pure HAP. However, the values of Debye-Waller factors σ^2 for both were significantly higher than that for the pure crystalline HAP, indicating considerable deviations in the atomic arrangement around the Ca atom in the two bone samples. In La-treated rats, the Debye-Waller factor was smaller than that in normal bone.

Dissolution Kinetics of Bone Mineral

The specific surface areas of the bone powders of normal and La-treated rats were 0.88 ± 0.08 and 0.90 ± 0.09 m^2/g, respectively. Since the same amount of bone powder (10.0 ± 0.2 mg) was used in the experiment for both normal and La-treated bone, the kinetic data were normalized for the surface area. Curves shown in Figure 2A and B are based on the averaged data of three independent measurements. The consumed HAc and the released Ca^{2+} were divided by total surface areas, respectively, and plotted against time. A steeper slope of the kinetic curve indicates a higher dissolving rate. These kinetic data show that the bone mineral of La-treated rats is more easily dissolved than that of normal bone.

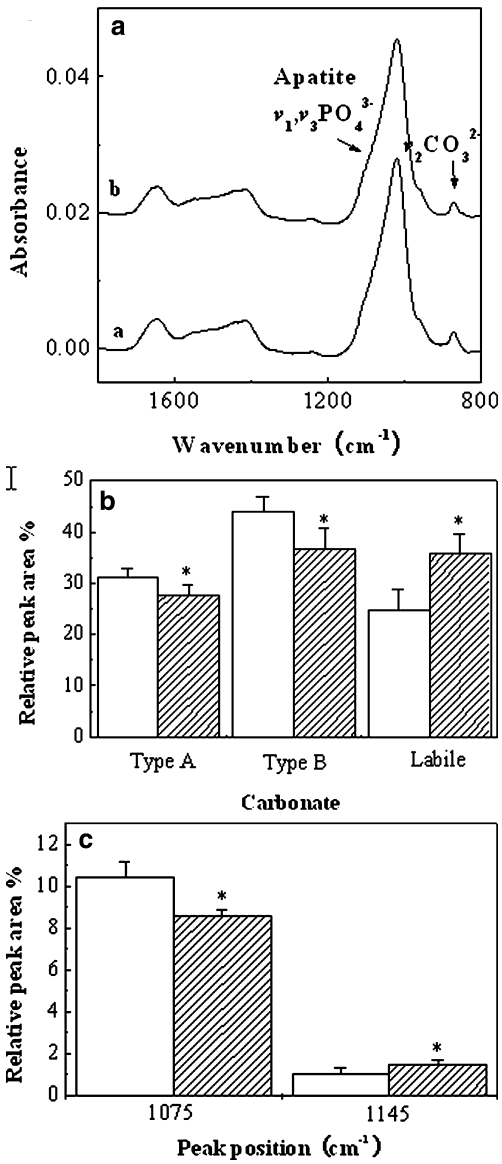

Fig. 1. La-caused changes in the amounts of carbonate and phosphate in bone mineral (mean ± SEM, $n = 8$; $^*P < 0.05$ indicates statistically significant differences.) (A) FT-IRM spectra (1,800–800 cm^{-1}) of normal (*a*) and La-treated (*b*) bones from the diaphysis of rat femur. The spectra of interest to the present study have been marked. (B) The percentages of type A, type B, and labile carbonates. Comparison was made between the results from curve fitting for CO_3^{2-} ν_2 vibrations of normal (*open bars*) and La-treated (*hatched bars*) bones. (C) La-caused changes in the relative crystal size and acid phosphate content. Comparason was made between the results from curve fitting for PO_4^{3-} ν_1 and ν_3 vibrations of normal (*open bars*) and La-treated (*hatched bars*) bones.

Discussion

The chemical composition, crystal structure, and short-range order of mineral crystals in bone play essential roles in the biological and structural functions of bone. Small changes in the mineral/collagen organization may considerably affect the biomechanical properties of bone. The data in Table 1, in addition to confirming the La accumulation in bone, revealed changes in bone composition. The decline in mineral content (described as mineral-to-matrix ratio) is consistent with the reduced Ca and P contents. Since the amount of bone-accumulated La is about eight orders of magnitude less than that of Ca and P, the disturbance of the molar ratio of Ca to P by substituting La^{3+} for Ca^{2+} is undetectable. The Ca-to-P ratio for normal bone is in agreement with values reported previously [28].

Crystal size is a key factor in bone metabolism and difficult to measure with enough accuracy by conventional methods. Both FT-IRM and SR-SAXS were used to estimate the crystal size of bone minerals. Values of size derived from FT-IR spectra are only relative [31], while SAXS provides more valuable information on crystal thickness [32], especially when the resolution is markedly increased by application of synchrotron radiation. Results from FT-IR and SR-SAXS measurements indicate reduced crystal thickness for the bone mineral of La-treated rats. Because the mineral-to-matrix ratio and crystal size reflect bone maturity [31, 33], the reduced thickness in combination with the declines in mineral content and Ca and P contents indicates that bone maturation was retarded by La treatment.

Carbonate is not a natural constituent of the HAP crystal but becomes incorporated into the OH (type A) and PO_4 (type B) lattice sites or adsorbed onto the HAP surface (labile carbonate) [29]. The content of labile carbonate (instead of total carbonate) is always used to correlate inversely with bone maturity [26, 29]. While type A and type B carbonates were reduced with the bone of La-treated rats, the amount of labile carbonate increased significantly, also suggesting retarded maturation of bone in La-treated Wistar rats.

Changes in states of phosphate were also observed. As indicated by the relative area of the peak at 1,145 cm^{-1}, the content of acidic phosphate (expressed as HPO_4^{2-}) increased in the mineral of La-treated bone. Because acidic phosphate is abundant in young bone and its content decreases as bone matures [34, 35], the higher content may also be associated with retarded bone maturation in La-treated rats. A positive correlation between unstable ("labile") carbonate and acidic phosphate was observed, in agreement with previously reported results [35].

The SR-EXAFS measurement generates parameters describing crystal lattice at the atomic level. The increased crystallinity, as indicated by the lower Debye-Waller factors in La-treated bone mineral, appears to contradict the notion that higher crystallinity is associated with bigger crystal size and greater maturity in natural bone [36]. However, taking into consideration the lower substitution of carbonate for hydroxyl and phosphate in HAP lattice with La-treated bone, the observed lower Debye-Waller factors (indicating less

Table 2. Structural parameters for the Ca *k* edges of bone samples and HAP (R = distance between calcium and neighbor atoms, σ^2 = Debye-Waller factor)

Shell parameter	Bond	Normal bone	La-treated	HAP[a]
R (Å) ± 0.02	Ca-6.6O	2.41	2.41	2.41
	Ca-2.4P	3.16	3.16	3.16
	Ca-2.4P	3.65	3.63	3.63
σ^2 (Å^2) ± 0.001	Ca-6.6O	0.036[b]	0.030[b,c]	0.025
	Ca-2.4P	0.035[b]	0.032[b,c]	0.027
	Ca-2.4P	0.043[b]	0.037[b,c]	0.020

[a] Analytical purity (Sigma, St. Louis, MO)
[b] Difference was considered significant ($P < 0.05$) between the same bonds in bone and HAP
[c] Difference was considered significant ($P < 0.05$) between the same bonds in La-treated and normal bone

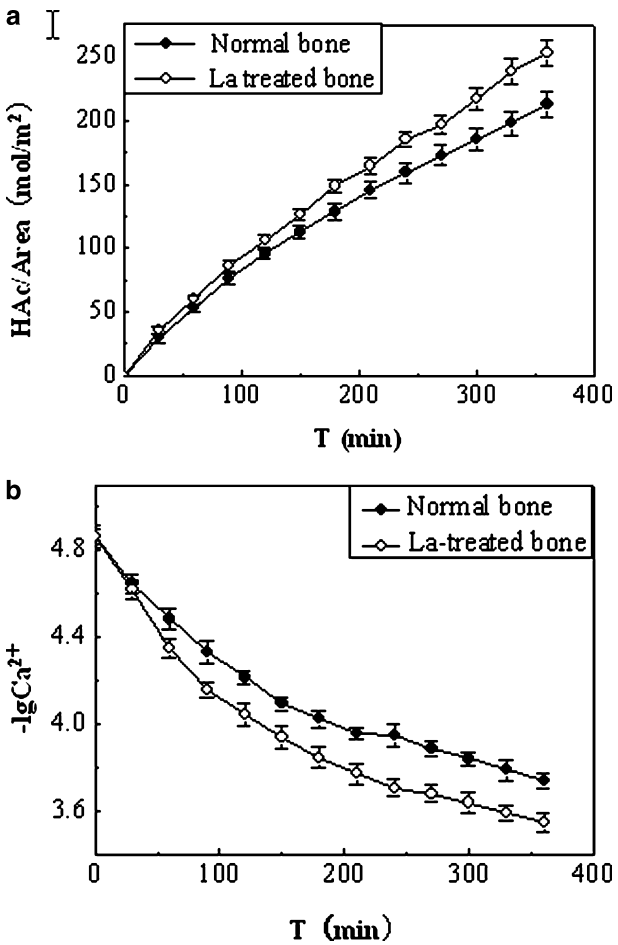

Fig. 2. Dissolution kinetics of bone mineral. (A) Plot of consumed HAc against time. (B) Logarithmic plot of released Ca^{2+} (mol · L^{-1}) against time. Values are means ± SEM.

lattice distortion compared to HAP) might be anticipated. Since reduced lattice carbonate (types A and B) correlates to increased labile carbonate (i.e., less bone maturity as discussed previously), the SR-EXAFS data provide further evidence for retarded bone maturation in La-treated rats. Because the Debye-Waller factor incorporates both dynamic and static disorder and both crystal size and carbonate substitution (types A Type B) may contribute to the latter [19], a lower Debye-Waller factor (thus a higher crystallinity) may not necessarily correspond to a larger crystal size and greater maturity. In fact, higher, lower, and the same degree of crystallinity have been reported for less mature bone [22, 34]. Hence, direct correlation of the Debye-Waller factor with crystal size and bone maturity seems not to be universally applicable.

The La-caused alterations of bone mineral, such as smaller size, more adsorbed labile carbonate, and more acidic phosphate, should make the bone mineral easier to dissolve, a phenomenon that we did observe (Fig. 2). In addition to the mineral composition, the crystal size and the lattice alteration, as revealed by SR-EXAFS, may contribute to the accelerated dissolution rate.

Recently, De Broe et al. [37] found that administration of high doses of $La_2(CO_3)_3 \cdot 4H_2O$ for 12 weeks brought no alteration in bone histomorphometry of animals with normal renal function. Such conflicting data may be the result of tissue heterogeneity, age, dietary influences, and physical activity. This disparity may also be attributable to the different instrumentation used to generate the data concerning the properties of bone.

The mechanism underlying the La-induced retardation of bone maturation remains unclear. Compared with the contents of Ca and P (Table 1), the amount of La accumulated in bone seems too small to exert any significant impact on the composition, microstructure, and dissolution property. An explanation of these findings is phosphate depletion induced by the La compound's powerful phosphate binding, resulting in decreased phosphate incorporation in bone. In addition, since bone is remodeled continuously during adulthood through the resorption of old bone by osteoclasts and the formation of new bone by osteoblasts and La^{3+} has been recognized to be a nonspecific blocker of Ca^{2+} channels [38], it is possible that La may affect cellular activities. *In vivo* study demonstrated that lanthanides can induce chromosomal aberrations in bone marrow cells and the number of aberrant cells increased with an increase in the concentration and period of treatment [39]. *In vitro* studies also showed that La influenced

bone-resorbing activity of rabbit mature osteoclasts [40]. Taking these facts and our findings into consideration, one can conclude that La may display its impacts through decreasing phosphate incorporation in bone and interfering with cellular processes followed by deposition in bone mineral.

Acknowledgment. This study was supported by National Natural Science Foundation of China (grants 20271005 and 20571006).

References

1. Sigel A, Sigel H (2003) Metal ions in biological systems, vol 40. Marcel Dekker, New York
2. Bulman RA (2003) Metabolism and toxicity of the lanthanides. In: Sigel A, Sigel H (eds) Metal ions in biological systems, vol 40. Marcel Dekker, New York, pp 683–706
3. Qi D, Chen L (1985) A spectrochemical study on the distribution of rare earth contents in plant. J Peking Univ (Nat Sci) 6:68–74
4. Chen Z, Liu Y, Wang Y (2000) Study on distributions and accumulations of rare earth element cerium (^{141}Ce) in mice. J Nanjing Agricult Univ 23:101–103
5. Zhu W, Xu S, Shao P, Zhang H, Feng J, Wu D, Yang W (1997) Investigation on intake allowance of rare earth: a study on bio-effect of rare earth in South Jiangxi. Chin Environ Sci 17:63–65
6. Pang X, Li D, Peng A (2002) Application of rare-earth elements in the agriculture of China and its environmental behavior in soil. Environ Sci Pollut Res Int 9:143–148
7. Ji YJ, Li JL (2000) Recent development in the study of biological effects of rare earth elements in China. J Health Toxicol 14:23–28
8. Wang K, Cheng Y, Yang X, Li R (2003) Cell responses to lanthanides and potential pharmacological actions of lanthanides. In: Sigel A, Sigel H (eds) Metal ions in biological systems, vol 40. Marcel Dekker, New York, pp 707–751
9. Helm L, Toth E, Merbach AE (2003) Lanthanide ions as magnetic resonance imaging agents. Nuclear and electronic relaxation properties. In: Sigel A, Sigel H (eds) Metal ions in biological systems, vol 40. Marcel Dekker, New York, pp 589–641
10. Albaaj F, Hutchison AJ (2005) Lanthanum carbonate (Fosrenol): a novel agent for the treatment of hyperphosphataemia in renal failure and dialysis patients. Int J Clin Pract 59:1091–1096
11. Behets GJ, Verberckmoes SC, D'Haese PC, Broe ME De (2004) Lanthanum carbonate: a new phosphate binder. Curr Opin Nephrol Hypertens 13:403–409
12. Vanholder R, Cornelis R, Dhondt A, Lameire N (2002) The role of trace elements in uremic toxicity. Nephrol Dial Transplant 17(suppl 2):2–8and references therein
13. Jarup L (2002) Cadmium overload and toxicity. Nephrol Dial Transplant 17(suppl 2):35–39
14. Wang K (1997) The analogy in chemical and biological behavior between non-special ions compared with essential ions. S Afr J Chem 50:232–238
15. Hardie MJ, Raston CL, Salinas A (2001) A 3,12-connected vertice sharing adamantoid hydrogen bonded network featuring tetrameric clusters of cyclotriveratrylene. Chem Commun 21:1850–1851
16. Jalilehvand F, Spångberg D, Lindqvist-Reis P, Hermansson K, Persson I, Sandström M (2001) Hydration of the calcium ion. An EXAFS, large-angle X-ray scattering, and molecular dynamics simulation study. J Am Chem Soc 123:431–441
17. Schaad Ph, Gramain Ph, Gorce F, Voegel JC (1990) Dissolution of synthetic hydroxyapatite in the presence of lanthanum ions. J Chem Soc Faraday Trans 86:4025–4029
18. Chen PS, Toribora TY, Warner H (1956) Microdetermination of phosphorus. Anal Chem 28:1756–1758
19. Peters F, Schwarz K, Epple M (2000) The structure of bone studied with synchroton X-ray diffraction, X-ray absorption spectroscopy and thermal analysis. Thermochim Acta 361:131–138
20. Fratzl P, Fratzl-Zelman N, Klaushofer K, Vogl G, Koller K (1991) Nucleation and growth of mineral crystals in bone studied by small-angle X-ray scattering. Calcif Tissue Int 48:407–413
21. Gadaleta SJ, Camacho NP, Mendelsohn R, Boskey AL (1996) Fourier transform infrared microscopy of calcified turkey leg tendon. Calcif Tissue Int 58:17–23
22. Harries JE, Hukins DW, Hasnain SS (1988) Calcium environment in bone mineral determined by EXAFS spectroscopy. Calcif Tissue Int 43:250–253
23. Gurman SJ, Binsted N, Ross I (1984) A rapid exact curved-wave theory for EXAFS calculations. J Phys C17:143–151
24. Grynpas MD, Cheng PT (1988) Fluoride reduces the rate of dissolution of bone. Bone Miner 5:1–9
25. Fratzl P, Schreiber S, Roschger P, Lafage M-H, Rodan G, Klaushofer K (1996) Effects of sodium fluoride and alendronate on the bone mineral in minipigs: a small-angle X-ray scattering and backscattered electron imaging study. J Bone Miner Res 11:248–253
26. Rey C, Renugopalakrshanan V, Collins B, Glimecher MJ (1991) Fourier transform infrared spectroscopic study of the carbonate ions in bone mineral during aging. Calcif Tissue Int 49:251–258
27. Nancy PC, Lindy H, Talyar RT, Alex W, Cory FB, Cathleen LR, Leon R, Adele LB (1999) The material basis for reduced mechanical properties in oim mice bones. J Bone Miner Res 14:264–272
28. Bohic S, Rey C, Legrand A, Sfihi H, Rohanizadeh R, Martel C, Barbier A, Daculsi G (2000) Characterization of the trabecular rat bone mineral: effect of ovariectomy and bisphosphonate treatment. Bone 26:341–348
29. Boskey AL, Gadaleta S, Gundberg C, Doty SB, Ducy P, Karsenty G (1998) Fourier transform infrared microspectroscopic analysis of bones of osteocalcin-deficient mice provides insight into the function of osteocalcin. Bone 23:187–196
30. Gadaleta SJ, Camacho NP, Mendelsohn R, Boskey AL (1996) Fourier transform infrared microspectroscopy of calcified turkey leg tendon. Calcif Tissue Int 58:17–23
31. Camacho NP, Rinnerthaler S, Paschalis EP, Mendelsohn R, Boshey AL, Fratzl P (1999) Complementary information on bone ultrastructure from scanning small angle X-ray scattering and Fourier-transform infrared microspectroscopy. Bone 25:287–293
32. Fratzl P, Groschner M, Vogl G, Koller K (1992) Mineral crystals in calcified tissues: a comparative study by SAXS. J Bone Miner Res 7:329–334
33. Shapses SA, Cifuentes M, Spevak L, Chowdhury H, Brittingham J, Boskey AL, Denhardt DT (2003) Osteopontin facilitates bone resorption, decreasing bone mineral crystallinity and content during calcium deficiency. Calcif Tissue Int 73:86–92
34. Huang RY, Miller ML, Carlson CS, Chance MR (2002) Characterization of bone mineral composition in the proximal tibia of cynomolgus monkeys: effect of ovariectomy and nandrolone deaconate treatment. Bone 30:492–497
35. Miller LM, Vairamurthy V, Chance MR, Mendelsohn R, Paschalis EP, Betts F, Bosky AL (2001) In situ analysis of mineral content and crystallinity in bone using infrared micro-spectroscopy of the ν_3 PO_4^{3-} vibration. Biochim Biophys Acta 1527:11–19

36. Paschalis EP, Betts F, DiCarlo E, Mendelsohn R, Boskey AL (1997) FTIR microspectroscopic analysis of normal human cortical and trabecular bone. Calcif Tissue Int 61:480–486
37. Behets GJ, Dams G, Vercauteren SR, Damment SJ, Bouillon R, De Broe ME, D'Haese PC (2004) Does the phosphate binder lanthanum carbonate affect bone in rats with chronic renal failure. J Am Soc Nephrol 15:2219–2228
38. Guo L, Davidson RM (1999) Extracellular Ca^{2+} increases cytosolic free Ca^{2+} in freshly isolated rate odontoblasts. J Bone Miner Res 14:1357–1366
39. Anand MJ, Akhilesh CS (1995) Clastogenicity of lanthanides: induction of chromosomal aberration in bone marrow cells of mice *in vivo*. Mutation Res 341:193–197
40. Zhang JC, Xu SJ, Wang K, Yu SF (2003) Effect of the rare earth ions on bone resorbing function of rabbit mature osteoclasts *in vitro*. Chin Sci Bull 48:2170–2175